LCC-0103
UCRL-JC- 149787
September 2002

Linear Collider Collaboration Tech Notes

Characterization of W-26% Re Target Material

A.J. Sunwoo, D.C. Freeman, W. Stein,
Lawrence Livermore National Laboratory
Livermore, CA

V. K. Bharadwaj , D. C. Schultz, J. C. Sheppard

Stanford Linear Accelerator Center
Stanford, CA 94309, USA

Abstract: The power deposition of an incident electron beam in a tungsten-rhenium target and the resultant thermal shock stresses in the material have been modeled with a transient, dynamic, structural response finite element code. The Next Linear Collider electron beam is assumed split into three parts, with each part impinging on a 4 radiation lengths thick target. Three targets are required to avoid excessive thermal stresses in the targets. Energy deposition from each beam pulse occurs over 265 nanoseconds and results in heating of the target and pressure pulses straining the material. The rapid power deposition of the electron beam and the resultant temperature profile in the target generates stress and pressure waves in the material that are considerably larger than those calculated by a static analysis. The 6.22 GeV electron beam has a spot radius size of 3 mm and results in a maximum temperature jump of 147°C. Stress pressure pulses are induced in the material from the rapid thermal expansion of the hotter material with peak effective stresses reaching 83 ksi (5.77×10^8 Pa) on the back side of the target, which is less than one half of the yield strength of the tungsten/rhenium alloy and below the material fatigue limit.

UCRL-JC- 149787
Preprint
LCC-0103

Characterization of W-26% Re Target Material

A. J. Sunwoo, D. C. Freeman, W. Stein,
V. K. Bharadwaj, D. C. Shultz, J. C. Sheppard

This paper was prepared for submittal to

Particle Sources Working Group
Snowmass, CO
July 6-10, 2001

September 10, 2002

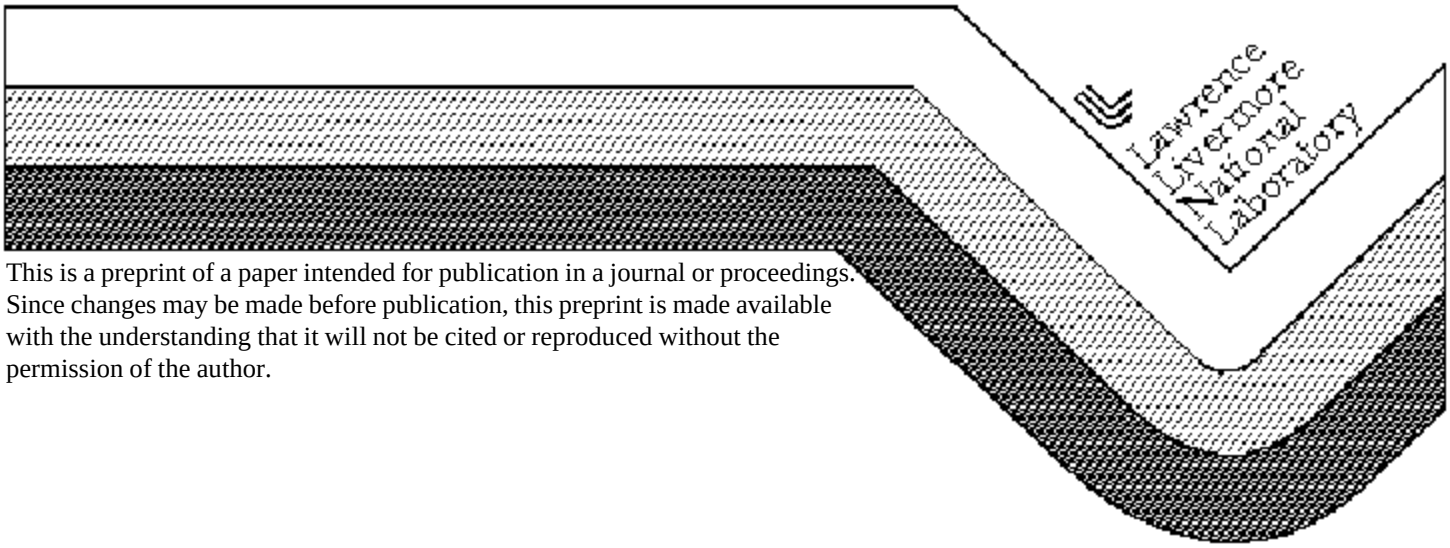

Characterization of W-26% Re Target Material

A. J. Sunwoo[1], D. C. Freeman[1], W. Stein[1],
V. K. Bharadwaj[2], D. C. Shultz[2], J. C. Sheppard[2]
[1]Lawrence Livermore National Laboratory, 7000 East Ave, Livermore, CA 94550
[2]Stanford Linear Accelerator Center Stanford University, Stanford, CA 94309

Abstract

The W-26 wt-% Re alloy was selected as a Stanford Linear Collider (SLC) target material for its exceptional physics properties and for the high strength and good ductility at the anticipated target operating temperatures, above the DBTT. After several years of operation, the target failed catastrophically. A detailed microstructural and mechanical characterization of the non-irradiated disk indicates that the material has been PM processed, nonuniformly mechanically worked and stress relieved. As a result, the ductility of the material varies through the thickness of the disk, making it difficult to determine the DBTT. The results of tensile and fatigue properties are reported with the corresponding fractography of the fracture surfaces.

Introduction

Different from a typical use of tungsten (W)-rhenium (Re) alloys, the W-26 wt-% Re alloy was selected as a Stanford Linear Collider (SLC) target material for its exceptional physics properties and for the high strength and good ductility at the anticipated target operating temperatures [**Reuter and Hodgson**]. The operating temperatures between 115 and 330°C are substantially above the reported ductile to brittle transition temperature (DBTT) of the alloy. Not anticipated was the effect of the electron irradiation-induced damage on the material. After several years of operation, the target failed catastrophically [**Bharadwaj**]. A terse characterization of the failed target led to conclusion that the failure mechanism was thermal fatigue due to the cyclic thermal stress imposed by the nonuniform shower energy deposition of the incident 33 GeV electron beam [**DeStaebler**].

Irradiation damage on the materials is well documented [**Bailat** *et al*]. In the case of the SLC target, possible causes of failure could be from the continuous bombardment of a nonuniform incident of 33 GeV electron beam. Enough energy is produced to dislodge atoms from their lattice sites to form clusters of atoms [**DeStaebler**]. The consequential interrelated effects are the increased DBTT and decreased mechanical properties [**Barabash** *et al*]. Clustering of atoms, coupled with increased temperature, could promote the formation of brittle sigma and chi precipitates along grain boundaries, decreasing the ductility of the alloy and reversing the beneficial effects of Re in W [**Nemoto** *et al*].

Because of the high melting temperature and the low temperature intrinsic brittleness of W-Re alloys, the processing varies between arc melting and powder metallurgy (PM) techniques depending on the applications. Both techniques are employed to produce the SLC target material. There are advantages and disadvantages for both processes. It is not well documented when the transition from the arc melting to the PM technique had taken place. The purpose of work was to characterize the microstructure of the current, non-irradiated W-26% Re target material to ascertain the processing history and determine the DBTT, and tensile and fatigue properties as a function of temperature.

Experimental Procedure

We obtained a 70-mm diameter by 25-mm thick W-26% Re disk from the Stanford Linear Accelerator Center (SLAC). To characterize the initial microstructure of the as-received disk, both cross-sectional and through-thickness surfaces were polished employing a standard polishing technique.

The surfaces were etched in a diluted solution of 10% NaOH in water at 1.5 VDC to bring out the microstructural features. Corresponding Vickers microhardness profiles were taken from the edge to the center and from the top to the bottom of the polished surfaces by applying a 100g_f load.

The tensile behavior of the alloy was determined by using miniature tensile specimens. A schematic of specimen locations on the disk and the dimensions are illustrated in **Figure 1**. The use of miniature specimens enabled us to extract a sufficient number of them from the through thickness direction. The specimens were produced using electrical discharge machining. Because of the hardness of the W-Re surfaces and the size of the specimens, gripping the specimens became extremely difficult. To enable the serrated grips of the test fixture to mechanically grip the specimen, and to prevent any potential slippage during testing, foils of malleable Ni were vacuum brazed to both sides of the specimen's gripping areas at 980°C for 5 minutes. Niora (82% Au and 18%Ni) was used as a braze alloy.

Furthermore, to ensure no slippage during testing, the specimens were preloaded in special sub-press to 28.9 kN compression for grip marks. The tensile tests were performed on a servo-hydraulic mechanical testing machine with a universal alignment fixture in an environmental chamber. Specimen displacement was measured with one extensometer across the sample width. Extensometer gage length was 5 mm.

The tensile tests were performed as a function of temperature and location in the disk. The ductile-brittle transition temperature of the alloy was determined by testing at temperatures ranging from 0 to 300°C. Tests performed at 150 and 300°C were done in an argon environment to prevent oxidation. The argon

environment is established by purging the chamber for 15 minutes before the temperature is turned on and continues during testing. Specimens are typically soaked at the target temperature for 10 minutes before testing. All tests were conducted at an initial strain rate of 4.2×10^{-3}/s. All tensile specimens were pulled to failure. At least three specimens were tested for each temperature. The fracture surfaces were viewed using a scanning electron microscope.

The fatigue behavior of the alloy was determined by simple fatigue stress vs. fatigue life (S-N) tests. The tests were performed under the guideline of ASTM E466. The set-up consisted of an environmental chamber and high temperature hydraulic grips to conduct testing at 300°C. Fatigue tests were performed on a computer controlled servo-hydraulic test machine, while the specimen was locally purged with argon. Smooth-bar, tapered specimens were taken diagonally from the disk, where the dimensions are illustrated in **Figure 1**. The specimen design followed the ASTM E466 5.0 specification for an hourglass specimen with a continuous radius. Similar to the tensile specimens Ni sleeves were vacuum brazed onto the ends of the specimen to maximize gripping during testing. The specimens were axially loaded at a ratio of R=-1 and cycled at 30Hz frequency. The specimens were tested with fully reversed cycling loading stresses of 589, 689 and 938 MPa. These stresses were selected because they were 50, 60, and 80% of UTS at 300°C, predetermined from earlier tensile tests. Tests were interrupted when the specimens did not break after 10^7 cycles.

Results

Microstructural Characterization

The microstructural characterization of the disk in the in-plane orientation reveals that the grain size is ASTM #4, having a nominal grain diameter of 90µm. However, each grain contains several subgrains. The microstructure from the

edge to center of the disk is displayed in **Figures 2 and 3**. Note that the micrographs were taken using a phase interference contrast technique. The jaggedness of grain boundaries helped to confirm that the disk material was PM processed. Another confirmation was the presence of randomly dispersed micropores, voids coupled with cracks outlining the grain boundaries, as evidently shown in **Figure 4.** It is inevitable that the material will fail intergranularly.

In the out-plane orientation, the grain size was ASTM #6, having a nominal grain diameter of 45μm. **Figures 5 and 6** compare the grain morphology in two directions (in- and out-plane). The micrographs were taken from the near outer and the middle section of the disk. The appearance of the grains suggests that the material has been extruded after sintering, but not recrystallized. However, the extrusion process may not have been uniform since the average Vickers hardness measurements indicate that the outer surfaces are much harder than at the middle, 580 vs. 525 kg/mm^2, respectively. These values are equivalent to the values reported for a stress-relieved condition [**Materials**]. This suggests that this particular W-26% alloy disk is an extruded, stress-relieved PM material [**Materials**]. The grain size and hardness vary with the degree of mechanical deformation received.

Having said that a caveat to the PM process is the production of a homogeneous W-26 wt-% Re alloy. The powders of W and Re have to be well blended prior to sintering. The results of chemical microprobe analyses for the W and Re distribution of the disk indicate that there was no apparent trend in the Re from the edge to the middle. Instead, it varied randomly from 22 to 28%. However, there was about 3 wt-% of material that is not accountable, which could be the impurity elements. High concentrations of impurity elements will have a

detrimental effect on the mechanical properties of the materials. A qualitative energy dispersive x-ray spectroscopy (EDS) on the specimens indicates that there was a subtle difference in Re content from the top to the middle, 26 vs. 28%, respectively.

As seen in **Figures 2-4**, the primary problem associated with the PM process is that the material contains microporosity along grain boundaries [**Lowery** and Asai]. Consequently, their presence weakens the grain boundary cohesion and causes premature brittle failure under a normal loading condition. **Ramalingam** et al reported that their sintered PM material contained 8% porosity. Because this value seems exceptionally high, various density measurement methods were employed to determine the density of the present material. The results of the study are reported in **Table 1**. The methods included a simple weigh and dimensional measurement, water immersion, and multi-pycnometry using helium as the reference gas. The benefit of the latter method is that it measures the changes in pressure and volume in the controlled, known conditions. Helium can diffuse into the fine open pores where water cannot. However if the alloy contained only closed pores, than He cannot effectively diffuse into the material for the given conditions. **Figure 7** clearly shows the presence of voids and grain boundary separation, which is more than adequate for He to diffuse into. The differences in density values from the calculated and measured results determine the presence of microporosity in the material. This particular disk contains about 2-3% porosity, which corresponds closely to the microprobe results.

A diffusion bonding study conducted by **Nieh** using a Ni interlayer showed that the formation of a Ni-W-Re ternary alloy can cause embrittlement in the parent material by nucleating at the grain boundary. The cross-sectional view of a

tensile specimen in a grip region, shown in **Figure 7**, reveals that vacuum brazing of a Ni foil using Niora had no adverse effect on the integrity of the specimen. On the other hand, Cu should be avoided since it does have an embrittling effect on the parent material. Interface strength for the W-Cu composites is low because of a lack of mutual solubility, compared to those of the W-Re alloys [**Belk** *et al*].

Tensile Properties

The results of tensile tests are given in **Table 2. Figure 8** plots the strength as a function of temperature and specimen location. As expected, the strength of the alloy decreased with increasing temperature. The rate of decrease was not linear. There were two precipitous decreases from 0 to 25°C and from 90 to 150°C. The strength of the alloy was not sensitive to the specimen location. A corresponding plot of elongation and reduction in area as a function of temperature is displayed in **Figure 8**. The overall ductility of the alloy was the lowest at 25°C. These values were even lower than the ones at 0°C. However, the specimen location had a substantial influence on the ductility of the alloy. **Figure 9** exhibits a plot of elongation sensitivity of the alloy as a function of location and temperature. Consistent in all temperatures, the specimens taken from the softer middle region of the disk exhibited considerably higher elongation values than the ones taken the near outer surface. At 25°C, the ductility of the material can vary from 11% to 3%, respectively. These results suggest that the outer layers of the disk will undergo a ductile-brittle transition at 25°C, while the middle region maintains ductile even at 0°C. Apparent differences in the ductility could be attributed to nonuniform mechanical deformation of the disk during processing.

The three specimens tested at 25°C display noticeably different tensile deformation profiles, as shown in **Figure 10**. In the elastic region, the specimens behaved the same. A deviation was seen after the on set of plastic deformation. A ductile specimen from the middle section of the disk exhibited some degree of the yield-point phenomenon, where a drop to lower yield stress is gradual, remaining higher than the other two specimens. The specimen ultimately failed at the necking instability, which occurs at about 10% strain. The yield-point phenomenon was observed in all temperatures with the specimens that exhibited high elongation values. It appears that this energy release allowed the material to further deform. As the temperature increases to 90°C and higher, the specimens tend to deform beyond necking instability, where the ultimate tensile strength remained typically at 10% strain. In comparison, the specimens from the outer surfaces tend to fail before necking. The curves are highly serrated which could be attributed to impurities and microporosity present in grain boundaries hindering the mobility of dislocations.

Fractography

The differences in the tensile response can be elucidated from the representative fracture surfaces. **Figures 11-13** compare the fracture surfaces of specimens, exhibiting different elongation values at 25°C and 150°C. Although the fracture surfaces of W-Re alloy do not exhibit typical ductile, microvoid coalescence, the specimens that had some ductility displayed a very fine, uniformly delaminated, intergranular fracture that ultimately failed in a shear mode. It appears as though there is less resistance to dislocation mobility in the in-plane direction than in the out-plane direction. Intergranular fracture in the PM material is expected due to the presence of microporosity. It appears that formation of a multilayer delamination is beneficial for the tensile response of the alloy, possibly improving its ductility. For the less ductile specimen, the

presence of the multiplayer delamination was not seen. Instead the fracture surface revealed a brittle, cleavage fracture mode. The specimen failed bluntly.

The differences in fracture characteristics became more obvious with the increased temperature. The ductile fracture surfaces continued to display interlocking, highly deformed grains. The less ductile surfaces displayed wedge-shaped (W-type) intergranular cracks, typically seen in high temperature fractured specimens at which the cracks are initiated by grain boundary sliding [**Shin** *et al*].

Fatigue Properties

At all temperatures, a ratio of UTS/YS for the W-Re alloy response under stress control indicates softening, since the ratio is less than 1.2 (see **Table 2**) [**Smith** *et al***,** and **Hertzberg**]. Cyclic softening is a particularly severe condition because the constant stress range produces a continually increasing strain range response, leading to early fracture [**Hertzberg**]. Thus, when the specimen was stress loaded to 80% of the 300°C UTS value, it failed after 10^4 cycles. When the cyclic stress decreased to 50% of the UTS, the specimen did not break even after 10^7 cycles. When the cyclic stress increased to 60% of UTS, it failed after 10^7 cycles. With a few data points, we can only conjecture that the thermal fatigue endurance limit of 10^{7+} cycles for this particular material at 300°C is 600 MPa. The results of fatigue tests are summarized in **Table 3**.

Discussion

The innate nature of the bcc crystalline materials cannot be completely changed but with alloying additions and process optimization, the microstructure and mechanical properties can be improved. The hcp lattice structured Re is added

to the bcc lattice structured W to improve its ductility and to lower the DBTT since Re retains its ductility from subzero to high temperatures [**AMP**]. Equally important is to stress relieve the recrystallized PM material which tends to have much higher DBTT than the stress relieved PM material, 380 and 215°C, respectively [**Lowery** and Asai]. In the W-Ni-Fe alloy, **Bussiba** *et al* found that the degree of plastic deformation positively influenced the DBTT. A lower DBTT seen in highly deformed material was attributed to the increased fracture stress of the grains, which enabled further plastic deformation without failure. The deformation mechanism for the W alloys is a screw dislocation [**Ohrinder**] and the high activation energy of the screw dislocation makes nucleation difficult. Extensively worked material generates sufficient populations of screw dislocations to surpass initial yielding. However, this benefit becomes eradicated if the adhesion strength between adjacent grains is weak such that intergranular separation occurs before the onset of plasticity.

A W-10% Re alloy that underwent PM processing, swaging, rolling, and stress relieving displayed a similar tensile response at 20°C and at 250°C as the W-26% Re alloy that underwent an equivalent processing history [**Krutwasser** *et al*] at the same temperatures. Determined by three-point bending tests, the DBTT of this material was 30 °C. Predictably, at 20°C the specimens broke prematurely, exhibiting less than 2% strain.

Lassila and LeBlanc conducted a series of tensile tests as a function of temperature and strain rate on the PM processed unalloyed W and W-5% Re alloy to obtain the basic tensile property data, DBTT, and strain rate sensitivity exponent. Their work showed that for a given material, the DBTT was significantly higher under dynamic loading and that alloying with Re lowered

the DBTT under quasi-static loading conditions. However, under dynamic loading the difference in the DBTT of the two materials was almost zero.

Another manufacturing process of W-Re alloys is vacuum arc remelt (VAR). Although the as-cast material tends to have a larger grain size than the PM material, the final product has fewer impurities and has no microporosity at grain boundaries. As a result, it is able to sustain extensive wrought processing. When the tensile properties PM processed W-26% Re alloy were compared to those produced by the arc cast and hot-rolled processed W-25% Re alloy (**Table 4**) [**Vandervoort**], the present material exhibited greater than 10% lower strength for given two temperatures. The reduction in area was also substantially lower in comparison. Similarly, the VAR material exhibits superior ductility and lower DBTT (35°C), whereas the PM material transitions at higher temperature (130°C) {**Wah**].

In addition to mechanical property advantages, the vacuum arc melt processed alloy has the greater resistance to the irradiation damage. **Matolich** *et al* studied the effects of Re addition and processing on the resistance to fast neutron fluence damage. They selected two materials: a commercial purity W metal that has been sintered, swaged and recrystallized and the high purity W-25% Re alloy that has been vacuum arc melted, extruded, hot swaged and recrystallized. The immersion density and dimensional measurements distinctly showed that the addition of Re suppressed swelling in all temperatures ranging between 400 and 1100°C. The swelling caused by irradiation of the W metal reached a peak at about 750°C. A lack of swelling seen in the W-25% Re alloy was attributed to the precipitation of a second phase, which hindered void formation. Unfortunately, because they varied two controlling factors simultaneously, it is difficult to individualize which was the primary contributor.

The transmission electron microscopy characterization of the same irradiated arc cast W-25% Re alloy revealed that the second phase formed is the ? -Mn phase (WRe_3), instead of the ? phase [**Sikka** and Moteff]. The kinetics of the irradiation-induced precipitation of the ? -Mn phase could be enhanced by the atom displacements. It is believed that the collision cascade produces the regions in the alloy that favor a Re atom rich core, providing nucleation sites for the ? -Mn phase. Of the two phases, ? -Mn is less detrimental to the mechanical property of the material.

Correspondingly, the results of a simulation study by **Caturla** *et al*, suggest that in the SLC target the damage per incident electron is highly localized. Increased temperature will help the migration of defects and therefore increase recombination between defects. Although recombination between vacancy and interstitial type of defects will reduce the total defect concentration, on the other hand, it could result in precipitation of second phases that are beneficial and detrimental for the mechanical properties of these materials. Thus, irradiation induced precipitates cause both hardening as well as embrittling of the alloy. A reduction of the Re content should reduce the effects of the radiation embrittlement by limiting the presence of Re atom rich cores [**Nemoto** *et al*].

For future study, it is recommended that the alloy be fabricated using the VAR process with a lower Re content. The VAR process produced material exhibits full density, eliminating the detrimental presence of microporosity, voids, and cracks along grain boundary. It also provides irradiation damage resistance. Small amounts of Re addition are needed to increase ductility and improve workability. **Bryskin** and Carlen at Re industry, **Wah** Chang's Technical Report, and internal memo from **Plansee** indicate that the W-25% Re alloy susceptible to

high concentration of ?-phase had a much lower ductility, even after annealing treatment. Ductility of the alloy improved with 22-24% Re. To function as grain refiner, 0.25% of HfC should be added during casting to benefit the effects of fine grain size exhibiting higher yield strength and lower DBTT.

Summary

The microstructural and mechanical characterization of the disk indicates that the material has been PM processed, nonuniformly mechanically worked and stress relieved. Since ductility improves from 25 to 0°C, it is difficult to determine the DBTT for this material. At the anticipated target operating temperatures between 115 and 330°C, the ductility of the material varies from 10 to 25%. A similar tensile deformation behavior is observed at 300°C. At this temperature, the fatigue endurance limit is established, using 50% of UTS value.

Acknowledgement

This work was performed under the auspices of the U.S. Department of Energy by the University of California, Lawrence Livermore National Laboratory under Contract No. W-7405-Eng-48.

References

Adv. Mater. Proc., 159, 2001, 143.

C. **Bailat**, F. Groschel, M. Victoria, J. Nuc. Mater., 276, 2000, 283.

V. **Barabash**, G. Federici, M. Rödig, L. L. Snead, C. H. Wu, J. Nucl. Mater. 283, 2000, 138.

J.A. **Belk**, M.R. Edwards, W.J. Farrll, B.K. and Mullah, Powder Metall., 36, 1993, 293.

V. K. **Bharadwaj** et al, Proc 2001 Particle Accel. Conf., Chicago, June 2001, 2123.

B. D. **Bryskin** and J.C. Carlen, Mater. Manu. Proc., 11, 1996, 83.

A. **Bussiba**, H. Mathias, A. Landali, M. Klipiec, and Y. Katz, Israel J. Tech, 24, 1988, 703.

M. **Caturla**, R. Roesler, J. Marian, B. Wirth, W. Stein and A. Sunwoo, to be published, 2002.

D. L. **Davidson** and F. R. Brotzen, Acta Metall. 18, 1970, 463.

H. **DeSaebler**, SLAC Collider Note 21, 1980.

P. **Krutwasser**, H. Derz, and E. Kny, 77, 673

R. W. **Hertzberg**, Deformation and Fracture Mechanics of Eng. Mater., Wiley, NY, 1976, 491.

D. H. **Lassila** and M. N. LeBlanc, UCRL-JC-108913, 1991.

R. R. **Lowery** and G. Asai, USBM-RC-1274, 1967.

Materials Engineering, Penton, 12, 1987, 100.

J. **Matolich**, J. Nahm, and J. Moteff, Scripta Metall., 8, 1974, 837.

T. G. **Nieh.** J. Mater. Sci., 1989.

Y. **Nemoto**, A. Hasegawa, M. Satou, and K, Abe, J. Nuc. Mater., 283, 2000, 1144.

E. **Ohriner**, ORNL, Private Communication, 2001.

Plansee, Private Communication between B. Kieffer and R. I. Jaffee, 1961.

M. L. **Ramalingam**, S. Snir, and D.L. Jacobson, J. Mater. Eng., 9, 1988, 353.

E. M. **Reuter** and J. A. Hodgson, IEEE Particle Conf., SF, CA, 1991.

R. W. **Smith**, M. H. Hirschberg, and S. S. Manson, NASA TN D-1574, NASA 4, 1963.

K. S. **Shin**, A. Luo, B.L. Chen, and D.L. Jacobson, JOM, 8, 1990, 12.

V. K. **Sikka**, and J. Moteff, Met. Trans. A, 5, 1974, 1514.

Smithells' Metals Reference Book, 6th ed., E. A. Brandes, ed., Butterworths, 1983, 11-424.

R.R. **Vandervoort**, Memorandum, 1971.

Wah Chang Albany Corp. Tech. Info. 1967.

Table 1. Density measurements

	Density, g/cc	Possible porosity, %
Tungsten	19.3	-
Rhenium	21.04	-
Reported W-27% Re[1]	19.8	-
Reported W-25% Re[2]	19.7	-
Calculated W-26% Re	19.75	-
SLAC	19.35	2.06
LLNL	19.16	2.99

[1] Vacuum melted.

[2] Reported from Re Alloys.

Table 2. Average tensile properties of W-26% Re alloy tested as a function of temperature.

Test Temperature	°C	0	25	90	150	300
Reduction in Area	%	14	5	18	20	27
Elongation	%	12	5	18	21	19
Load @ .2% Offset	lbf	893	858	793	643	642
Yield Stress	ksi	222	209	196	158	159
Yield Stress	MPa	1530	1442	1349	1091	1094
Maximum Load	lbf	969	896	840	705	692
Ultimate Tensile Strength	ksi	241	218	207	173	171
Ultimate Tensile Strength	MPa	1659	1505	1428	1196	1178
Modulus of Elasticity	Msi	61	62	60	59	60
Modulus of Elasticity	GPa	417	425	412	406	414
Test Environment		air	air	argon	argon	argon
Head Travel	in/min.	0.048	0.048	0.048	0.048	0.048
Head Travel	mm/s	0.0200	0.0200	0.0200	0.0200	0.0200
Ratio of UTS/YS		1.09	1.04	1.06	1.09	1.08

Table 3. Fatigue properties of W-26% Re alloy at 300°C.

Specimens	Cyclic stress level MPa	N_f
1-1*	589	2.88E+07+
1-4	690	1.55E+07
2-1	943	1.90E+04

* Specimen did not break.

Table 4. Tensile properties of arc cast and hot rolled W-25% Re alloy as a function of temperature. (Vandervoort, 1971).

Temp, °C	Yield Strength MPa (ksi)	UTS MPa (ksi)	Elongation %	Reduction in Area %
25	1620 (235)	1724 (250)	12	35
300	1258 (182.5)	1327 (192.5)	12	35
500	1138 (165)	1224 (177.5)	12	35
700	1069 (155)	1172 (170)	12	35

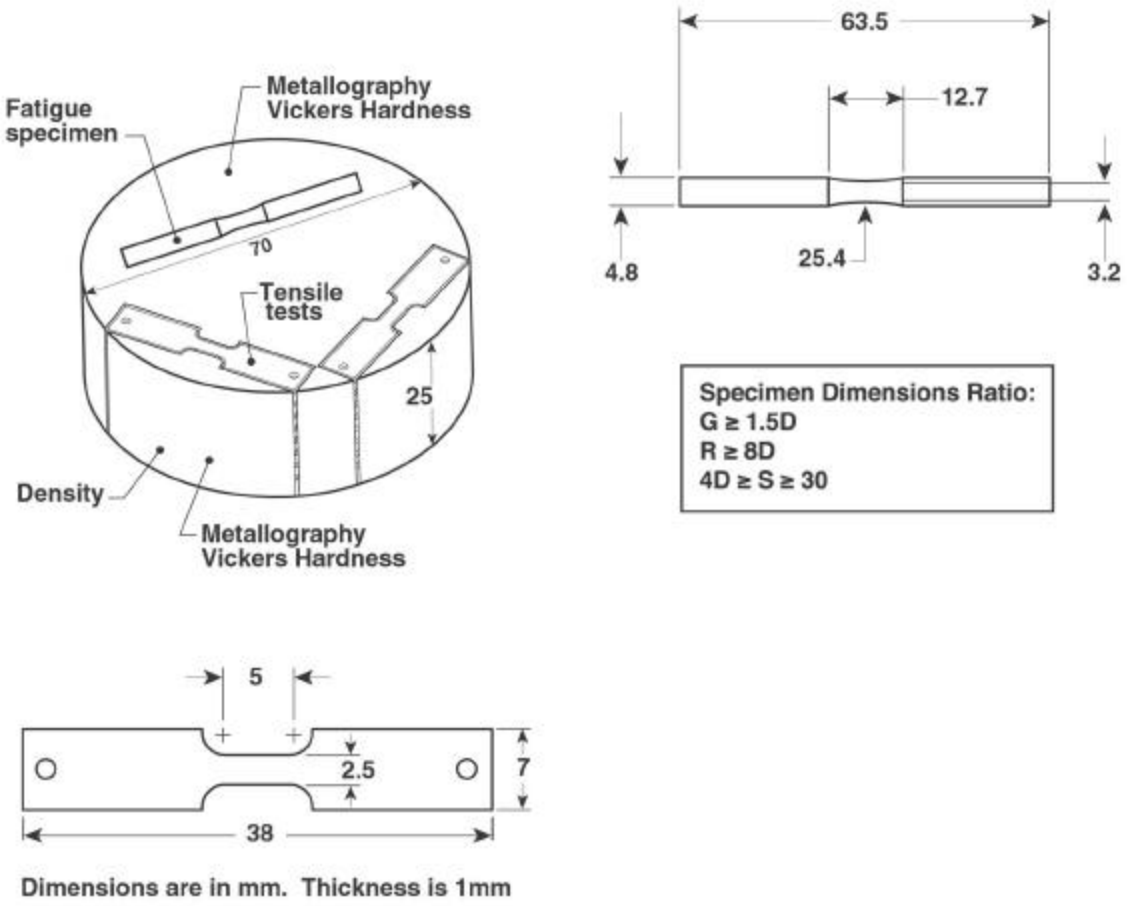

Figure 1. Schematics illustration of tensile and fatigue specimens and their locations in a 70-mm diameter by 25-mm thick W-26% Re disk.

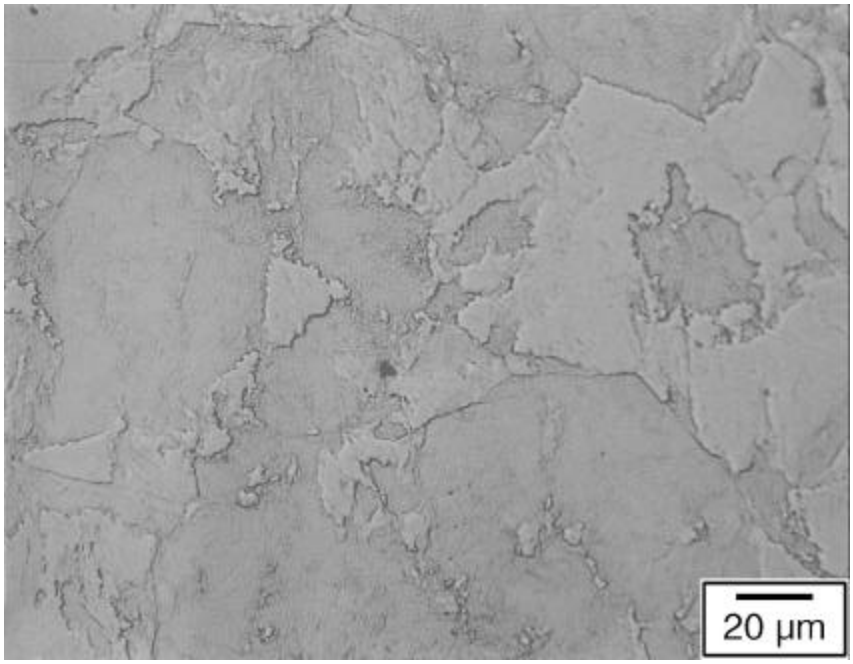

Figure 2. Cross-sectional view of the W-26% Re alloy taken near edge of the disk.

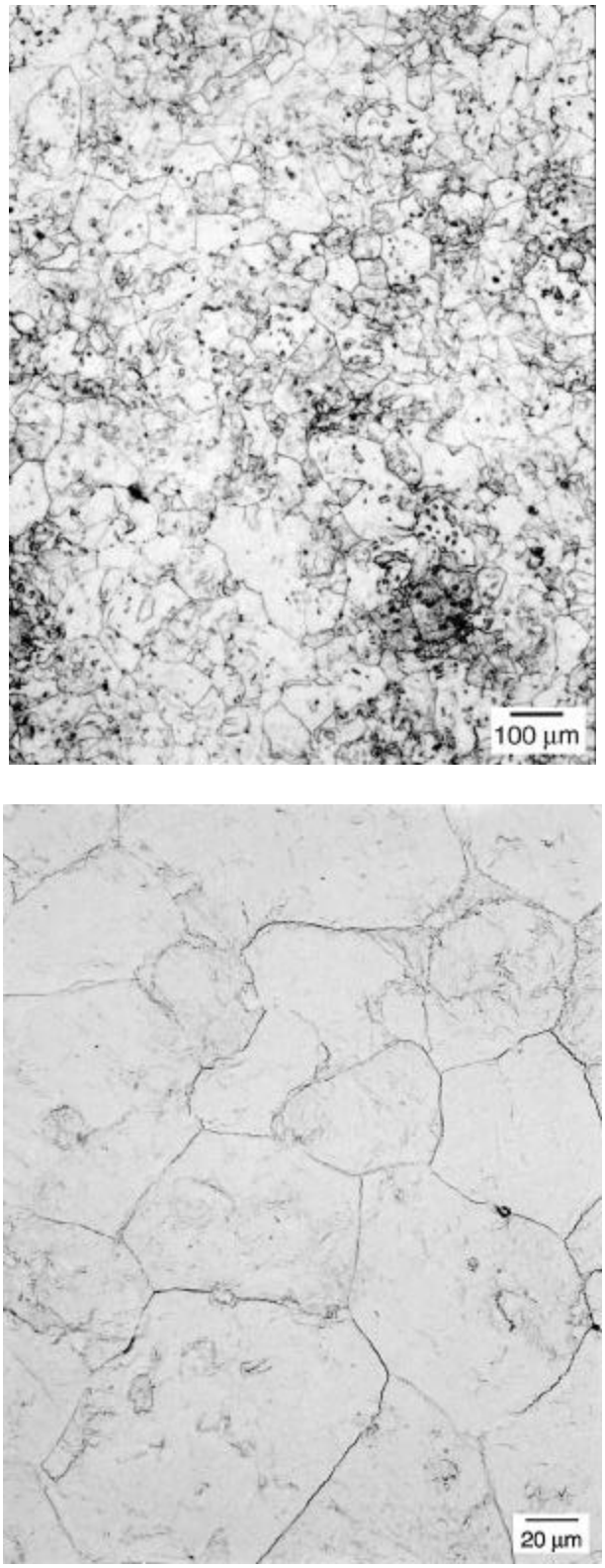

Figure 3. Cross-sectional view of the W-26% Re alloy taken near center at low magnification and high magnification.

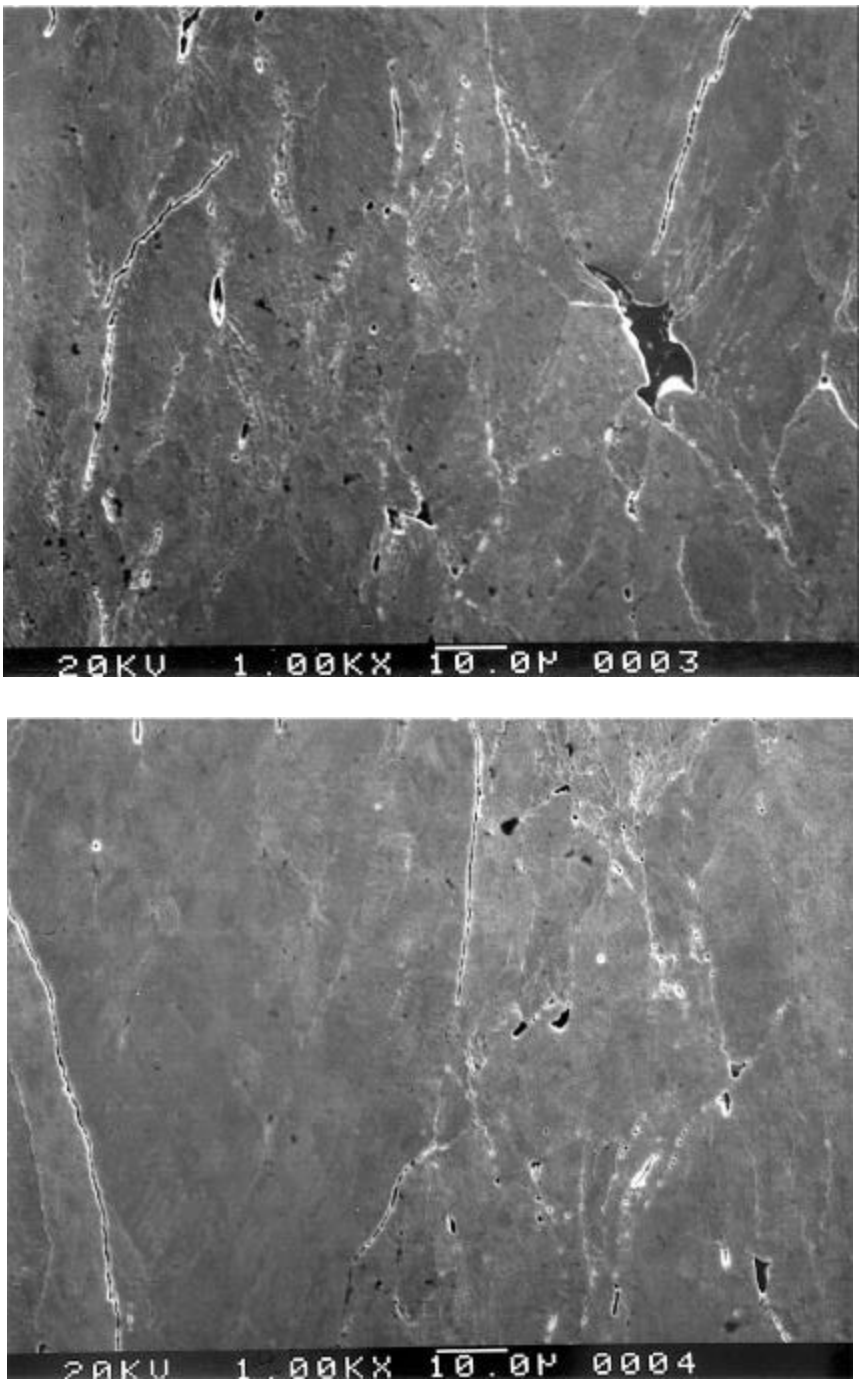

Figure 4. Scanning electron microscopy (SEM) micrographs of the W-26% Re alloy show the presence of micropores, voids and cracks outlining the grain boundaries.

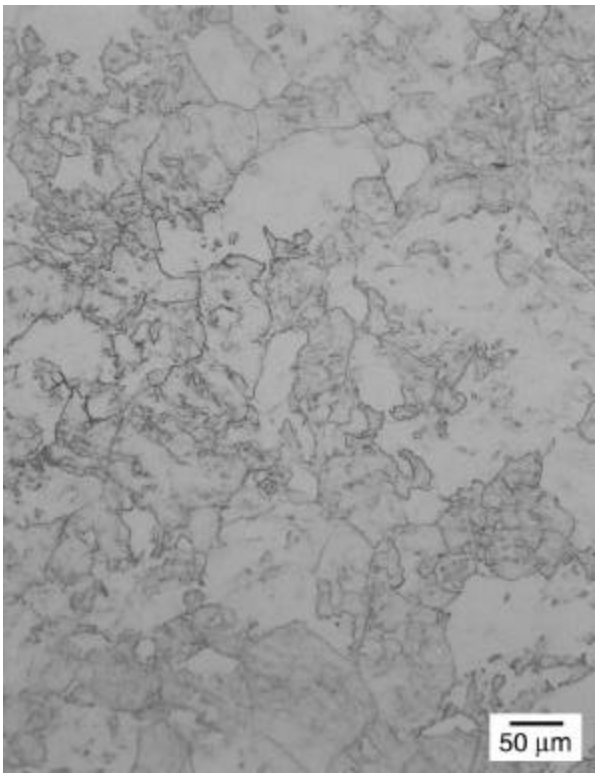
50 µm


50 µm

Figure. 5. Cross-sectional and edge view of the W-26% Re alloy taken near the outer section of the disk.

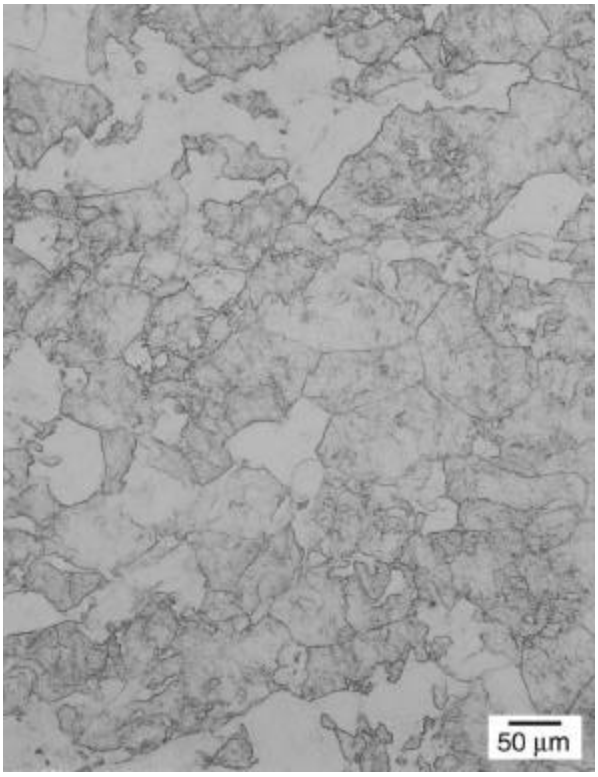
50 µm


50 µm

Figure 6. Cross-sectional and edge view of the W-26% Re alloy taken near the middle section of the disk.

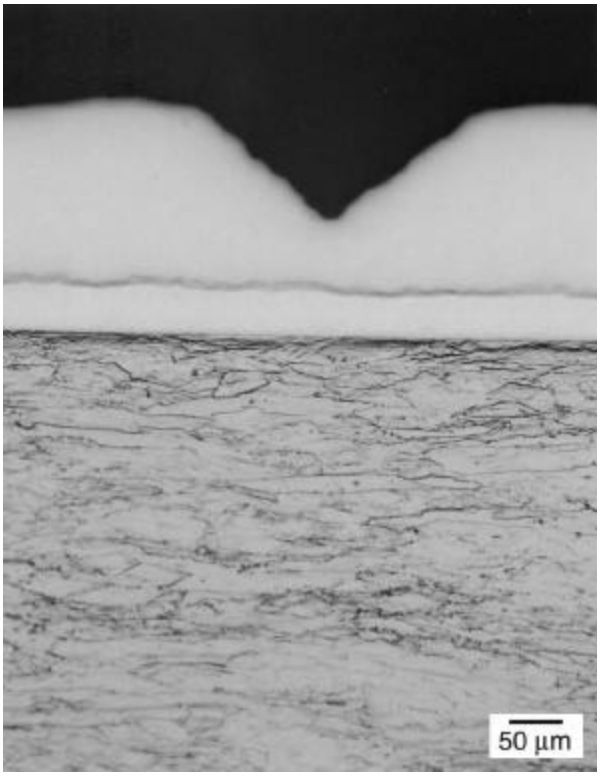

Figure 7. Cross-sectional view of the interfaces of W-Re, Niora, and Ni.

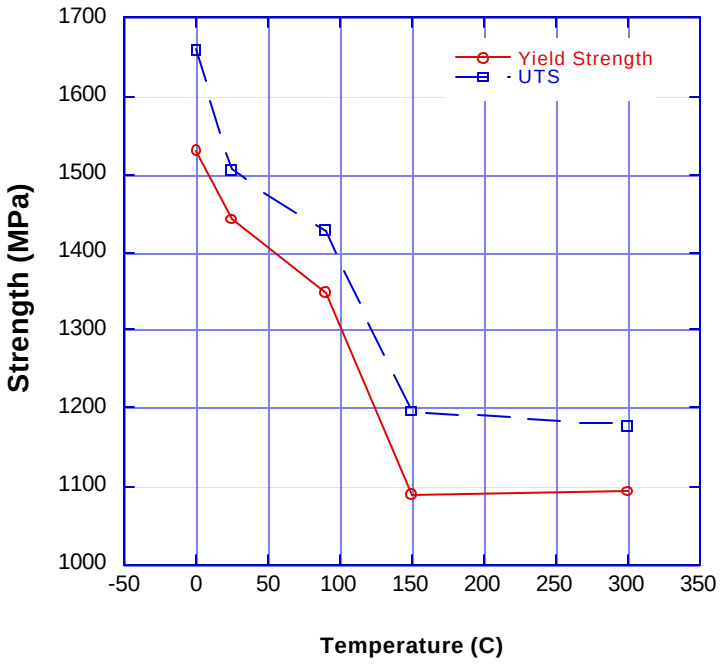

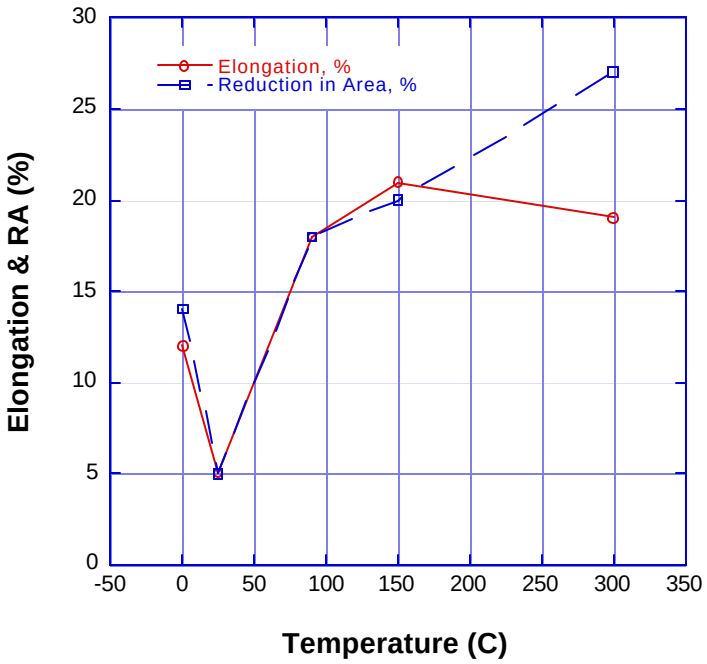

Figure 8. Tensile properties of W-26% Re alloy as a function of temperature.

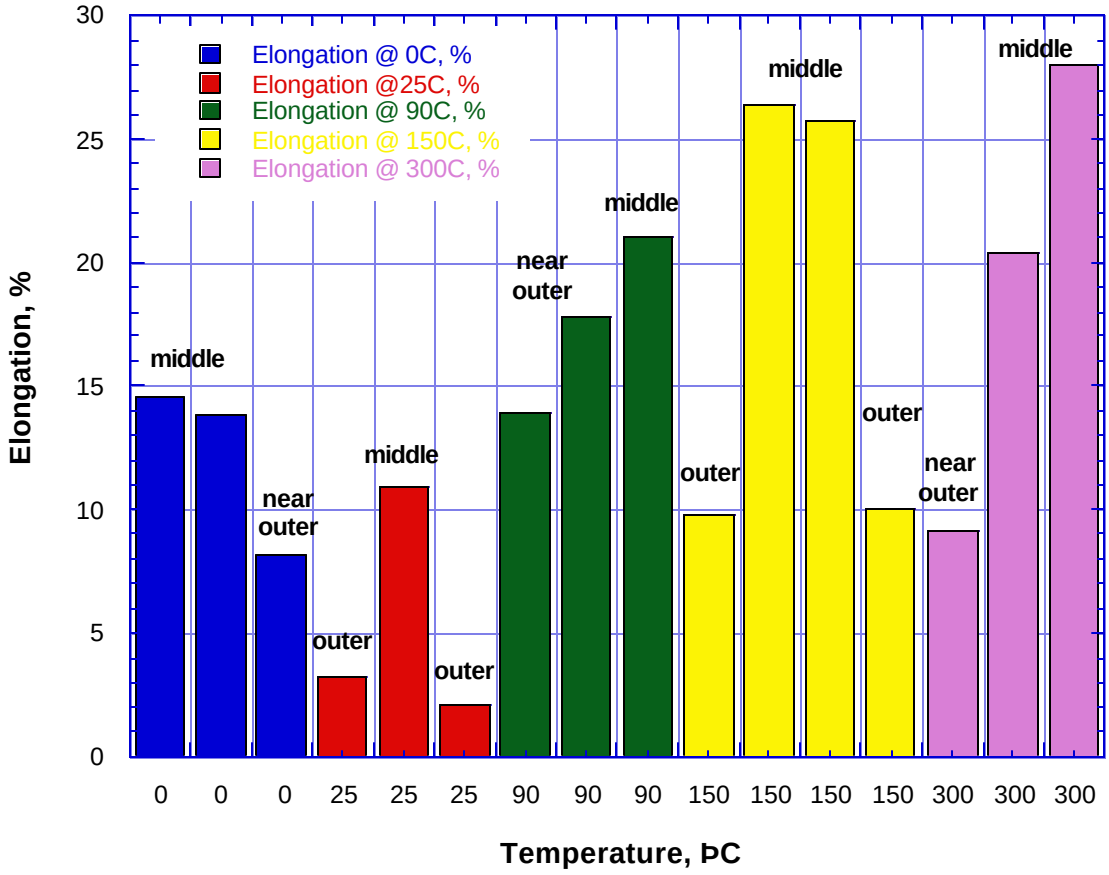

Figure 9. Effects of temperature and location on the ductility of the W-26% Re alloy disk.

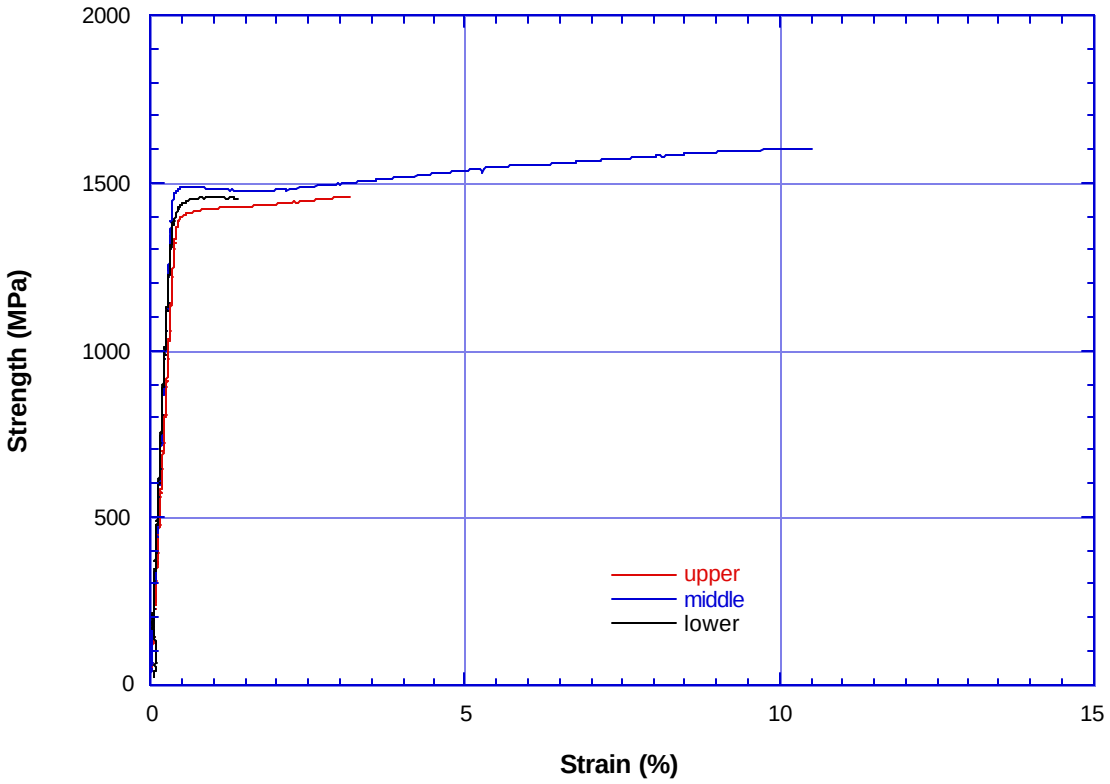

Figure 10. Stress-strain profiles of W-26% Re alloy. Specimens were obtained from different section of the disk and tested at 25°C in air environment at the strain rate of 10^{-3}/s.

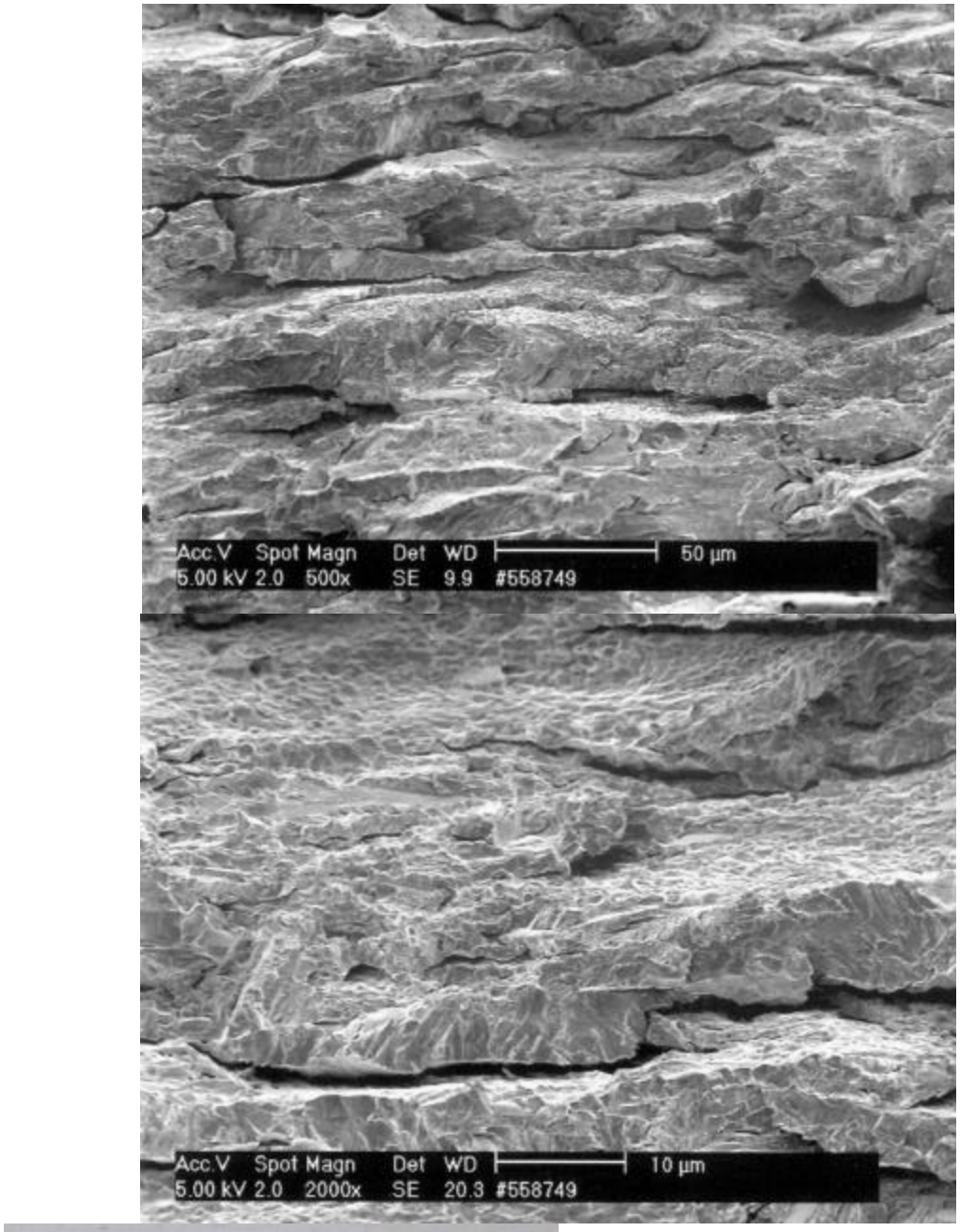

Figure 11. Fracture surfaces and cross-sectional view of a broken specimen tested at 20°C that exhibited high ductility.

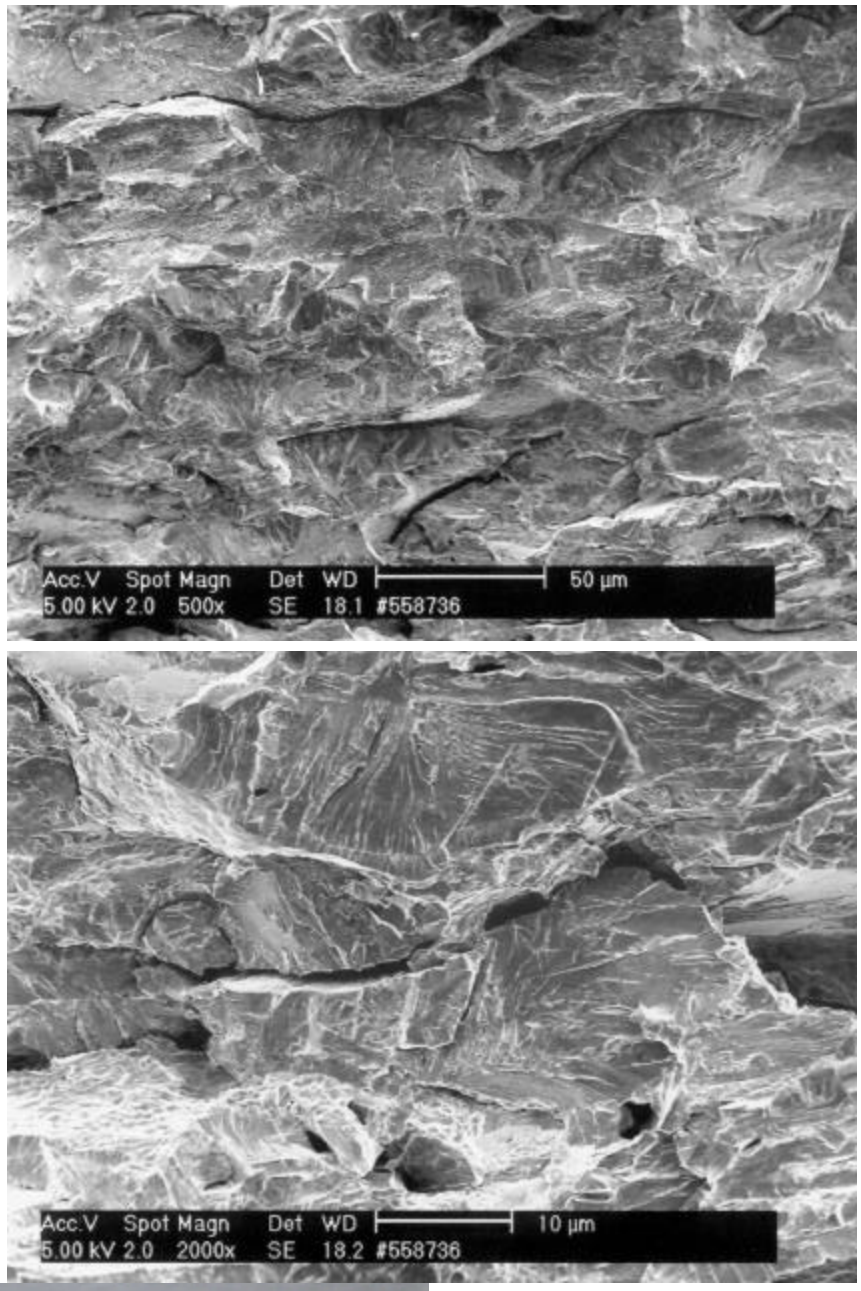

Figure 12. Fracture surfaces and cross-sectional view of a broken specimen tested at 20°C that exhibited low ductility.

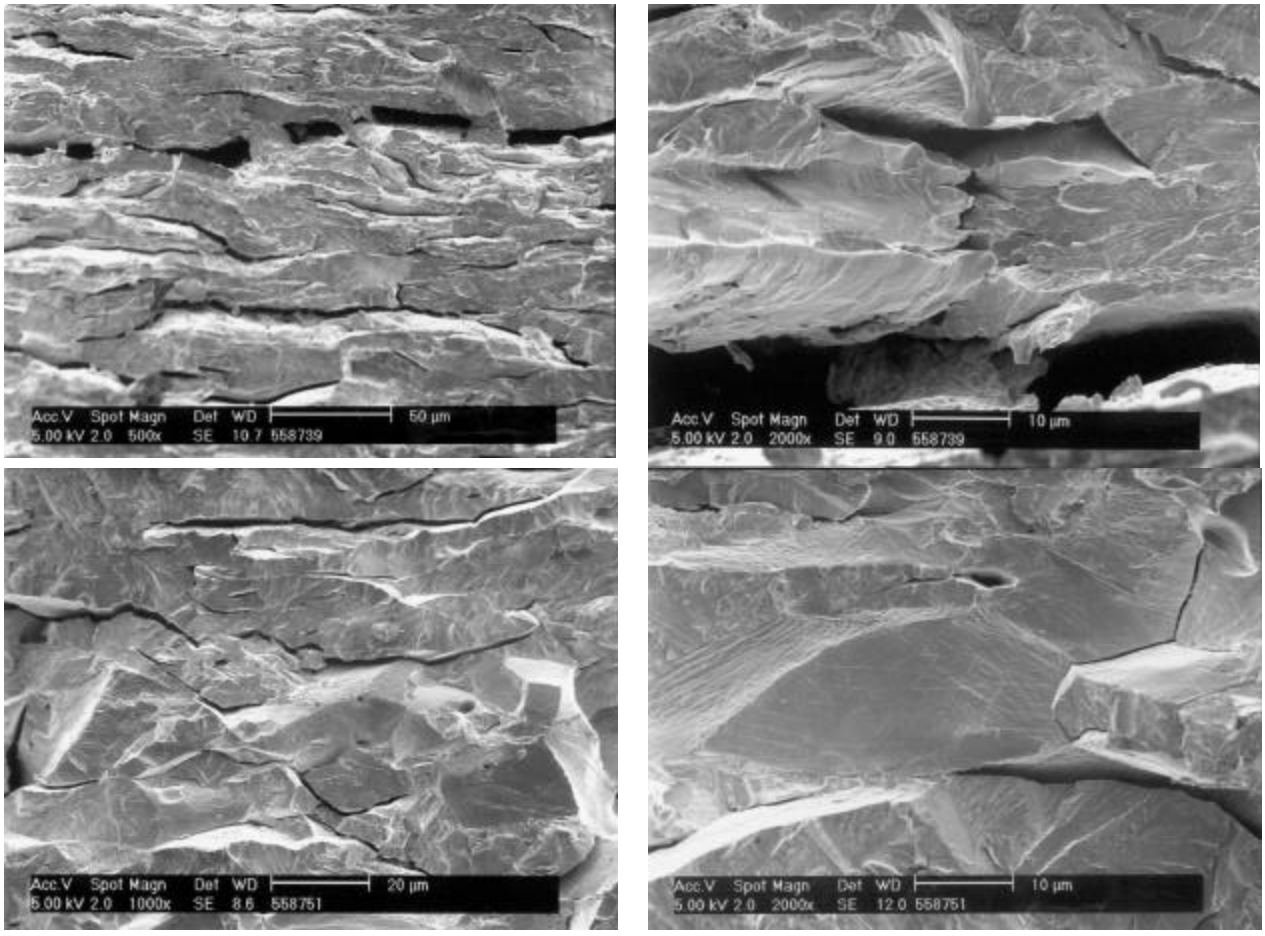

Figure 13. Effect of temperature on the fracture characteristics of W-Re specimens. Specimens were tested at 150°C. The upper specimen yielded 27% elongation compared to the lower specimen yielded only 10% elongation.

University of California · Livermore, California 94551